Dirty Paper Coding for Waveform Synthesis in Integrated Sensing and Communications: A Broadcast Channel Approach

Husheng Li

***Abstract*—In integrated sensing and communications (ISAC), both functions are tightly integrated using the same spectrum, waveform and hardware. Analogy is identified between ISAC and broadcast channel in communications, since ISAC transmitter broadcasts signals for both communication receivers and sensing, despite the functional overlap between communications and sensing. Although the communication signal can also be used for sensing, the intrinsic randomness of communications impairs the reliability of sensing. Therefore, a dedicated and deterministic sensing waveform is added, in order to improve the sensing performance. To remove the interference of the dedicated sensing waveform to communication receivers, dirty paper coding is employed, which exploits precoding for interference cancellation. Meanwhile, the trade-off between communications and sensing is identified. Numerical results are used to demonstrate the proposed ISAC scheme and the performance trade-off.**

I. Introduction

There is a resurrection of the technology of integrated sensing and communications (ISAC) since the development of the next generation (NextG) of wireless networks. It is a natural idea to integrate both functions in the same waveform and the same hardware platform, due to their similar frequency bands and radio frequency (RF) hardware architecture. When an ISAC transceiver sends out an electromagnetic (EM) wave, the forward signal brings data packets to the communication receiver, while the reflected EM wave carries the information of the reflector back to the ISAC transceiver. Therefore, the two functions of sensing and communications are accomplished in a single round of transmission. The ISAC technology resurges in recent years, due to the pressing demand from various cyber physical systems (CPSs), such as autonomous driving and unmanned aerial vehicles (UAVs), in which both communications and sensing are of critical importance.

A fundamental question in the study of ISAC is the conflict of interest between sensing and communications, as well as the quantification of the tradeoff. It has been found by the author in [1] that there is very little conflict in the different preferences of power spectral density (PSD) in the waveforms for sensing and communications, in terms of long-term performance. However, in the short-term performance, a major conflict is the uncertainty: on the one hand, randomness is essential for communications due to the uncertainty in the modulating data; on the other hand, sensing prefers deterministic waveforms that have been optimized in advance. As will be demonstrated in the numerical results, the sidelobes of the random data modulation are statistically higher than dedicated waveforms (e.g., the Golomb codes [2]).

H. Li is with the Department of Electrical Engineering and Computer Science, the University of Tennessee, Knoxville, TN (email: hli31@utk.edu, phone number: 865-974-3861, address: 312 Min Kao Building, 1520 Middle Drive, Knoxville, TN, 37996).

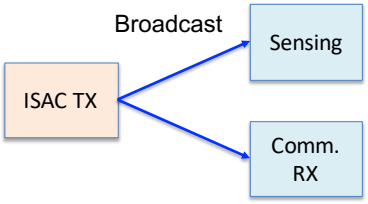

Fig. 1. Broadcast channel analogy of ISAC

In this paper, we propose to superimpose pure communication waveform x_c (with random data modulation) and deterministic sensing waveform x_s that help to shape the synthesized waveform $x = x_c + x_s$ and improve the sensing performance. For the purpose of sensing, both x_c and x_s benefit the sensing performance; therefore the whole signal x is used for sensing. However, for the purpose of communications, x_s is an interference to x_c, thus undermining the communication performance. We propose to use the technique of dirty paper coding [3], that eliminates the interference x_s to x_c at the communication receiver without extra power consumption, since x_s is known to the ISAC transceiver (but unknown to the communication receiver).

The major challenges for the proposed ISAC system, which are addressed in this paper, as well as the potential solutions, include

- How to eliminate the interference of x_s to the communication signal x_c? We will use lattice-based dirty paper coding to address this interference.
- How to assess the impact of x_c on the sensing performance? We will derive analytic expressions for the sensing performance in terms of the communication signal characteristics.

The application of dirty paper coding also implies the analogy of ISAC to broadcast channels in traditional communications, as illustrated in Fig. 1. One can consider the ISAC transmitter as broadcasting signals to the sensing receiver and communication receiver(s). The signals could be separated in the time (TDMA) or frequency (FDMA), or tightly integrated in the same waveform (such as the dirty paper coding). Therefore, various approaches developed in the study of broadcast channel can be applied. However, ISAC is different from the broadcast channel in communications: (a) the sensing receiver is not decoding the transmitted signal; instead, it 'decodes' the state of the channel (the target information); (b) the signal for communications

could also be useful for sensing, thus resulting in the overlap between functions of communications and sensing. These new challenges will be addressed in the context of ISAC.

The remainder of this paper is organized as follows. The related works are introduced in Section II. In Section III, the system model of ISAC is introduced. Then, the design of waveform superposition is discussed in Section IV, as well as the dirty paper coding for eliminating the interference of sensing waveform to the communication waveform. The power control for balancing communications and sensing will be studied in Section V. Numerical results and conclusions are provided in Sections VI and VII, respectively.

II. Related Works

In this section, we introduce works on ISAC and dirty paper coding related to this paper.

A. ISAC

For the technique of ISAC, comprehensive surveys can be found in [4]–[8]. Theoretical studies have been carried out for ISAC in [9]. Although the spatial separation of the two functions via beamforming [5], [7], [8] achieves higher spectral efficiency than the time/frequency separation, due to the reuse of the frequency spectrum, the mutual interference of communication and radar beams is still significant in practice [10], [11]. Moreover, when omni-directional communication or sensing is needed, or the sensed target and the communication receiver are co-located, the spatial separation is no longer valid. This justifies the nonlinear and inseparable waveforms. There are some such nonlinear and inseparable designs: the fractional Fourier transform is employed for waveform design [12]; in the mmWave band, the joint waveform design has been analyzed from the signal processing perspective in [13].

B. Dirty Paper Coding

Dirty paper coding, proposed and named in [3], is used to remove deterministic interference known to the transmitter (but unknown to the receiver). In more details, the transmitter needs to send out signal x subject to interference s. Then, the receiver receives signal $y = x + s + w$, where w is random noise. When s is unknown to both the transmitter and receiver, it can only be incorporated into the noise. However, when s is known to the transmitter, the receiver can completely remove the interference s by leveraging the dirty paper coding, even though it does not know s. Dirty paper coding is mainly used for the downlink broadcast of cellular systems. The base station, as the transmitter, needs to send messages to multiple receivers. Then, the message for one user can be considered as an interference for another user. Fortunately this interference is known to the base station, thus facilitating the dirty paper coding.

Taking the Tomlinson-Harashima scheme [14] for illustration, we assume that pulse amplitude modulation (PAM) is used for the modulation of x. The PAM constellatin is repeated, thus forming a lattice illustrated in Fig. 2. Since s is known to the communication encoder, we set $X_c = Q(s, x^0) - s$, where x^0 is the PAM symbol using normal modulation without considering s and $Q(s, x^0)$ is the lattice point corresponding to x^0 that is

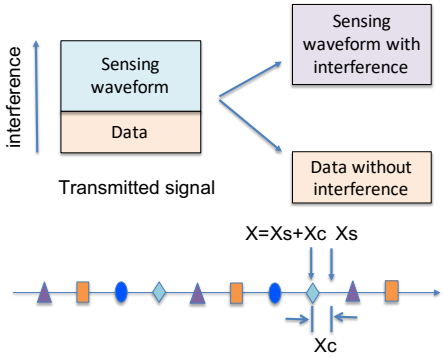

Fig. 2. An illustration of dirty paper coding in ISAC

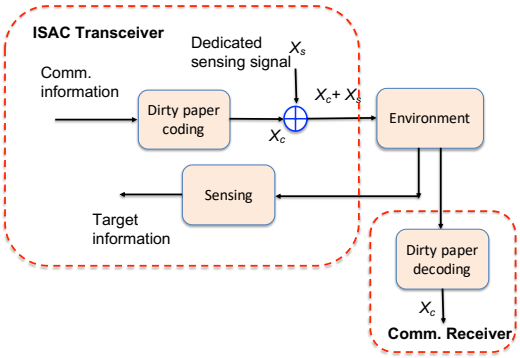

Fig. 3. System structure of dirty paper coding based ISAC

closest to s. Therefore, the transmitter sends out X_c and the receiver receives

$$X = s + X_c = Q(s, x^0). \tag{1}$$

Then, the communication receiver can figure out x^0 from the lattice and the received signal, while the total waveform X is still close to the interference s if the amplitude of X_c is small. The theoretical coding scheme can be found in [14]. It is applied in the downlink communications with multiple antennas [15], [16]. More practical coding schemes can be found in [17], [18].

III. System Model

We consider the orthogonal frequency division multiplexing (OFDM) waveform for the ISAC scheme, due to its wide applications in both communications and sensing. For simplicity, we consider single-antenna systems, although it will be very interesting to incorporate multiple antennas into the ISAC scheme. We assume N subcarriers with carrier frequency f_c and frequency gap δf between adjacent subcarriers. Therefore the signal within one OFDM symbol is given by

$$X(t) = e^{j2\pi f_c t} \sum_{n=0}^{N-1} X^n e^{j2\pi n \delta f t}, \qquad t \in [0, T_s], \tag{2}$$

where X^n is the complex symbol sent over the n-th subcarrier and T_s is the symbol period.

It is assumed that the ISAC receiver is operated simultaneously in a full-duplex manner. For simplicity, we assume point

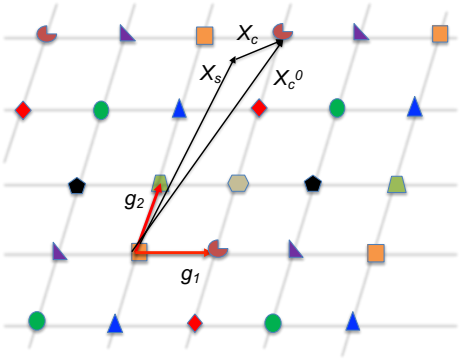

Fig. 4. Lattice based coding

target with significant reflections, if there is any. Therefore, the received signal is given by

$$Y(t) = \begin{cases} N(t), & \text{no target} \\ X(t-\tau) + N(t), & \text{target} \end{cases}, \tag{3}$$

where $N(t)$ is complex white Gaussian noise and τ is the round trip time of the signal. The total transmit power is denoted by P_t.

IV. Dirty Paper Coding Based ISAC

In this section, we introduce the proposed ISAC scheme based on dirty paper coding, whose structure is illustrated in Fig. 3, and the analogy to broadcast channel in communications.

A. Sensing Scheme

The transmitted signal on each subcarrier is layered. We assume that the symbol X^n is the superposition of communication symbols and sensing signal, namely

$$X^n = X_c^n + X_s^n, \tag{4}$$

where the superscripts c and s indicate communications and sensing, respectively. The communication signal X_c^n is encoded adaptively to the deterministic sensing signal X_s^n, while X_s^n is deterministic and could be optimized according to the statistical behavior of X_c^n. The encoding scheme and waveform optimization will be studied in the next subsections. The whole signal $\{X^n\}_{n=0,\dots,N-1}$ is used for radar sensing. We assume that the total transmit power P_t is divided into two parts, P_s for X_s and P_c for X_c, respectively, satisfying $P_t = P_s + P_c$. For simplicity, we assume that the channel is frequency-flat. Therefore, the communication power allocated to each subcarrier is given by $\frac{P_c}{N}$.

B. Dirty Paper Coding of X_c

We consider the coding over subcarrier n and omit the superscript n for notational simplicity. The dirty coding scheme is illustrated in Fig. 2, where the sensing signal X_s is placed at the top layer subject to the interference of the data signal X_c.

There have been substantial studies on the practical implementation of dirty paper coding in order to maximize the Gaussian vector broadcast channel capacity [16]–[18]. To shrink the gap between the performances of practical schemes and theoretical prediction, complex operations are needed, such as the constellation reshaping or trellis modulation. In this paper, as an initial exploitation of dirty paper coding, we consider the nested lattice code for the QAM modulation of each individual symbol, without involving the time domain variation, and will optimize the corresponding fundamental parallelogram (thus optimizing the sensing performance) in the subsequent subsection. For simplicity, we consider a 2-dimensional lattice in the IQ-plane [19]:

$$\Lambda_1 = \{\lambda = i_1\mathbf{g}_1 + i_2\mathbf{g}_2 : i_1, i_2 \in \mathbb{Z}\}, \tag{5}$$

where the vectors $\mathbf{g}_1$ and $\mathbf{g}_2$ are to be optimized. The constellation of the QAM symbol over each subcarrier is periodically repeated over Λ_1, as illustrated in Fig. 4. The points corresponding to each message m form a nested lattice $\Lambda_{2,m} \subset \Lambda_1$.

Similarly to the PAM case in Section II, we consider the quantization function $Q(X_s, m)$ which is defined as

$$Q(X_s, m) = \arg \min_{x \in \Lambda_{2,m}} \|x - X_s\|, \tag{6}$$

and the signal X_c is given by

$$X_c^m = Q(X_s, m) - X_s, \tag{7}$$

such that the ISAC transceiver sends out $Q(X_s, m)$.

C. Assessment of Sensing Performance

We now assess the sensing performance given the dirty paper coding scheme. In this paper, we consider minimizing the sidelobes of the autocorrelation function of the superimposed waveform. We use the integrated sidelobe level (ISL) [2] to characterize the radar sensing performance:

$$\xi = \sum_{k=-(N-1),k\neq 0}^{N_c-1} |r[k]|^2 = 2\sum_{k=1}^{N-1} |r[k]|^2, \tag{8}$$

where the autocorrelation function r is defined as

$$\begin{aligned} r(\tau) &= \int_{-\infty}^{\infty} x(t)x^*(t-\tau)dt \\ &= \int_{\tau}^{T_p} x(t)x^*(t-\tau)dt, \end{aligned} \tag{9}$$

and $r[k] = r(kT_c)$ is the k-th sample of the correlation function and $T_c = \frac{T_s}{N}$ is the chip period. For simplicity of analysis, we can approximate the signal $x(t)$ using the discrete-time chips:

$$x(t) \approx e^{j2\pi f_0 t} \sum_{n=0}^{N-1} x[n]p_n(t - nT_c), \tag{10}$$

where p_n is the rectangular pulse supported in $[0, T_c]$ and $\{x[n]\}_{n=0,\dots,N_c}$ are the inverse discrete Fourier transform (IDFT) of the subcarrier symbols $\{X^k\}_{k=0,\dots,N_c-1}$.

The following lemma, proven in another paper of the author [20], is needed for evaluating the ISL:

Lemma 1 ([20]). *The instantaneous ISL ξ of signals $\{X^k\}_{k=0,\dots,N-1}$ over N subcarriers, equals*

$$\xi = V[\{\Phi_p\}_{p=0,\dots,2N-1}], \tag{11}$$

where V is the variance, and $\{\Phi_p\}_{p=0,\dots,2N-1}$ is given by

$$\Phi_p = \begin{cases} |X^k|^2, & \text{if } p = 2k \\ |X \circledast Y(k)|^2, & \text{if } p = 2k+1 \end{cases}, \tag{12}$$

where $\circledast$ is the circular convolution, and Y is defined as

$$Y_m = \frac{2}{1 - e^{-j\frac{2\pi(2m+1)}{2N}}}. \tag{13}$$

Therefore, the optimization of the dedicated sensing waveform is formulated as

$$\min_{\{X_s^n\}_n} E\left[\xi | \{X_s^n\}_{n=0,\ldots,N-1}\right] \ s.t. \ \sum_{n=0}^{N-1} |X_s^n|^2 = P_s, \tag{14}$$

where the objective function is the expectation (over the random communication symbols) of the ISL, as a function of the dedicated sensing waveform, and the constraint is the power allocated to sensing. Note that the lattice Λ_1, determined by $\mathbf{g}_1$ and $\mathbf{g}_2$, is fixed, as well as the powers P_s and P_c. They will be optimized subsequently.

We need the following proposition for the finer structure of the objective function of ISL:

Proposition 1. *The expectation of the ISL is given by*

$$E[\xi] = \xi_s + E[\xi_c] + E[\xi_{s,c}] - \frac{2P_sP_c}{N^2}, \tag{15}$$

where ξ_s is the ISL of the sensing waveform (which is deterministic), ξ_c is the ISL of the communication waveform (which is random) and $\xi_{s,c}$ is the cross-term determined by both sensing and communication waveforms. Moreover, the expectation of ξ_c is given by

$$\begin{aligned} E[\xi_c] &= \frac{1}{2N}\left(\sum_{k=0}^{N_c-1} E|X_c^k|^4 + \sum_{p=0}^{N-1}\sum_{k=0}^{N_c-1} |Y_{(p-k)_N}|^4 E|X_c^k|^4 \right. \\ &+ \left. 2\left(\frac{P_c}{N}\right)^2 \sum_{p=0}^{N-1} \sum_{k_1,k_2=0,k_1\neq k_2}^{N-1} |Y_{(p-k_1)_N}|^2 |Y_{(p-k_2)_N}|^2 \right) \\ &- \frac{P_c^2}{N^2}, \end{aligned} \tag{16}$$

where $(x)_N = \mod(x, N)$ is the modular operation. The expectation of the cross-term $\xi_{s,c}$ is given by

$$\begin{aligned} E[\xi_{s,c}] &= \frac{2P_cP_s}{N} + 2\sum_{k_1=0}^{N-1} |Y_{(p-k_1)_N}|^4 |X_s^{k_1}|^2 \frac{P_c}{N} \\ &+ \sum_{k_1,_2=0,k_1\neq k_2}^{N-1} |Y_{(p-k_1)_N}|^2 |Y_{(p-k_2)_N}|^2 \\ &\times \frac{P_c}{N}\left(E|X_s^{k_1}|^2 + E|X_s^{k_2}|^2\right). \end{aligned} \tag{17}$$

Proof. First, for a general signal $\{X^k\}_{k=0,\ldots,N-1}$ with total power P, we obtain from (11) in Lemma 1

$$\begin{aligned} \xi &= \sum_{k=0}^{N-1} |X^k|^4 + \sum_{p=0}^{N-1} \left|\sum_{k=0}^{N-1} X^k Y_{(p-k)_N}\right|^4 - \frac{P^2}{N^2} \\ &= \sum_{k=0}^{N-1} |X^k|^4 - \frac{P_s^2}{N^2} - \frac{P_c^2}{N^2} - \frac{2P_sP_c}{N^2} \\ &+ \sum_{p=0}^{N-1}\left(\sum_{k_1=0}^{N-1} X^{k_1} Y_{(p-k-1)_N} \sum_{k_2=0}^{N-1} (X^{k_2})^* Y^*_{(p-k_2)_N}\right)^2 \end{aligned} \tag{18}$$

where the third term is further given by

$$\begin{aligned} &\sum_{k_1=0}^{N-1} X^{k_1} Y_{(p-k-1)_N} \sum_{k_2=0}^{N-1} (X^{k_2})^* Y^*_{(p-k_2)_N} \\ &= \sum_{k_1=0}^{N-1} |X^{k_1}|^2 |Y_{(p-k-1)_N}|^2 \\ &+ 2\sum_{k_1,k_2=0,k_1\neq k_2}^{N-1} Re\left[X^{k_1} Y_{(p-k-1)_N} (X^{k_2})^* Y^*_{(p-k_2)_N}\right] \end{aligned} \tag{19}$$

We substitute $X^k = X_s^k + X_c^k$ into the expression of ξ in (18) and obtain the first term

$$\begin{aligned} &E\left[\sum_{k=0}^{N-1} |X^k|^4\right] \\ &= \sum_{k=0}^{N-1} |X_s^k|^4 + E\left[|X_c^k|^4\right] + 2|X_s^k|^2 E\left[|X_c^k|^2\right] \\ &= \sum_{k=0}^{N-1} \left(|X_s^k|^4 + E\left[|X_c^k|^4\right]\right) + \frac{2P_cP_s}{N} \end{aligned} \tag{20}$$

and the third term

$$\begin{aligned} &E\left[\left(\sum_{k_1=0}^{N-1} X^{k_1} Y_{(p-k_1)_N} \sum_{k_2=0}^{N-1} (X^{k_2})^* Y^*_{(p-k_2)_N}\right)^2\right] \\ &= \sum_{k_1=0}^{N-1} E|X^{k_1}|^4 |Y_{(p-k_1)_N}|^4 \\ &+ \sum_{k_1,_2=0,k_1\neq k_2}^{N-1} E|X^{k_1}|^2 |Y_{(p-k_1)_N}|^2 E|X^{k_2}|^2 |Y_{(p-k_2)_N}|^2. \end{aligned} \tag{21}$$

We then substitute $E|X_k|^2 = |X_s^k|^2 + \frac{P_c}{N}$ into (21), and obtain the fourth order term

$$\begin{aligned} &\sum_{k_1=0}^{N-1} E|X^{k_1}|^4 |Y_{(p-k_1)_N}|^4 \\ &= \sum_{k_1=0}^{N-1} |Y_{(p-k_1)_N}|^4 \left(|X_s^{k_1}|^4 + E\left[|X_c^{k_1}|^4\right] + 2|X_s^{k_1}|^2 \frac{P_c}{N}\right), \end{aligned} \tag{22}$$

and the quadratic term

$$\begin{aligned} &\sum_{k_1,_2=0,k_1\neq k_2}^{N-1} E|X^{k_1}|^2 |Y_{(p-k_1)_N}|^2 E|X^{k_2}|^2 |Y_{(p-k_2)_N}|^2 \\ &= \sum_{k_1,_2=0,k_1\neq k_2}^{N-1} |Y_{(p-k_1)_N}|^2 |Y_{(p-k_2)_N}|^2 \\ &\times \left(E|X_s^{k_1}|^2 E|X_s^{k_2}|^2 + \frac{P_c}{N}\left(E|X_s^{k_1}|^2 + E|X_s^{k_2}|^2\right) + \left(\frac{P_c}{N}\right)^2\right). \end{aligned} \tag{23}$$

Summarizing (18), (20), (21), (22) and (23), we obtain the decoupled ξ_s and $E[\xi_c]$ and the cross-terms. The calculation of $E[\xi_c]$ is omitted due to the limited space. □

We noticed that the expected ISL is the sum of the ISLs of the sensing waveform and communication waveform, in addition to a cross-term. Therefore, to minimize the ISL, the sensing waveform needs to be optimized adaptively to the communication symbols. Numerical approaches can be devised

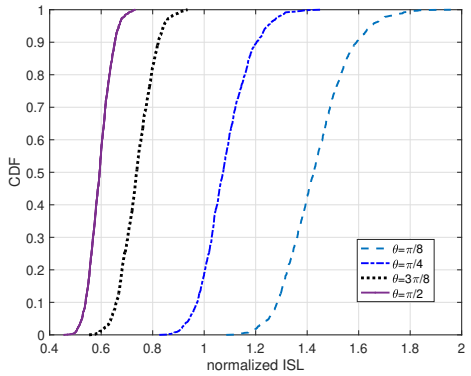

Fig. 5. Comparison between different lattice shapes

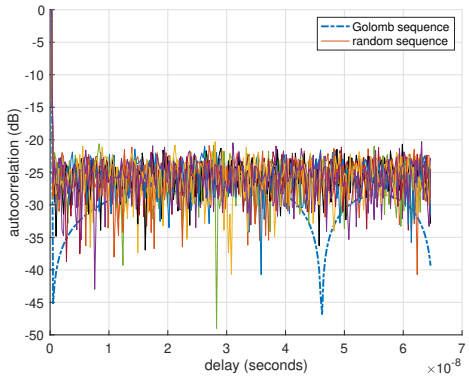

Fig. 6. Comparison between Golomb codes and OFDM waveform with random modulation.

to optimize the expected ISL, similarly to that in [2], which will be our future research. When the power of X_s is large, compared with that of X_c, the overall waveform $X_s + X_c$ is the quantized version of X_s, with respect to the lattice formed by X_c. Therefore, existing sensing waveforms with small ISL, such as the Golomb code or the Zadoff-Chu code [2], can be directly applied in such situations, which will be demonstrated by our numerical results.

D. Lattice Shaping

From Prop. 1, we observe that the expected cross-term $E[\xi_{s,c}]$ does not depend on the waveform of X_c, except for the power P_c allocated to communications. Therefore, to minimize the expected ISL, one simply minimizes the ISL $E[\xi_c]$ of the communication waveform. An analytic optimization is difficult. Therefore, we carried out numerical computations for different values of the angle θ between the vectors $\mathbf{g}_1$ and $\mathbf{g}_2$, where the modulation is 256QAM, and 256 subcarriers are assumed. We observe that the ISL is minimized when $\mathbf{g}_1$ and $\mathbf{g}_2$ are orthogonal. Therefore, in our subsequent analysis and simulations, we consider rectangular fundamental parallelograms.

V. Power Allocation

In this section, we study the power allocation to balance the powers P_s and P_c for sensing and communications, respectively. To this end, we formulate the following optimization problem:

$$\begin{aligned} & \max_{P_s} M \log\left(1+\frac{P_t-P_s}{M\sigma_n^2}\right) \\ s.t. \quad & E\left[\xi|\{X_s^n\}_{n=0,\ldots,N-1}\right] \le \gamma_\xi \\ & \sum_{n=0}^{N-1} |X_s^n|^2 = P_s, 0 \le P_s \le P, \end{aligned} \tag{24}$$

where γ_ξ is the threshold for the ISL and σ_n^2 is the communication receiver noise power. The rationale for the formulation is as follows: (a) Sensing: In typical situations, stringent constraints are placed for the radar sensing, since it is usually used for critical missions (e.g., collision avoidance in autonomous driving). (b) Communications: Compared with radar sensing, communication is more elastic, thus being set as the objective function for the best effort.

Thanks to the isolation of communication performance from the sensing waveform, resulted by the dirty paper coding, we can search for the value of P_s that meets the constraint of ISL and leave the remaining power to communications. This is summarized in Algorithm 1, given that the threshold γ_ξ can be achieved when all power is allocated to sensing.

Algorithm 1 Power Allocation for ISAC with Dirty Paper Coding

1: Initialize P_s.
2: **for** Constraint not met **do**
3: Increase P_s by a small step δP.
4: Use (1) to calculate the ISL $E[\xi]$.
5: **if** The ISL $E[\xi]$ is less than γ_ξ **then**
6: Allocate P_s and $P - P_s$ to sensing and communications, respectively. Break.
7: **end if**
8: **end for**

VI. Numerical Simulations

In this section, we provide numerical simulation results to demonstrate the performance of the proposed ISAC algorithm.

A. Dedicated Waveform vs. Random Waveform

Figure 6 shows the autocorrelation functions of the Golomb codes (designed for radar sensing) [2] and the OFDM waveform with random data modulation (superposition of 50 realizations), where we observe much lower sidelobes of the dedicated Golomb codes. Therefore, the waveform for ISAC should achieve a good tradeoff on the uncertainty between communications and sensing. In the subsequent simulations, we use the Golomb code for the sensing waveform X_s.

B. ISL Performance for Dirty Paper Coded Signals

In Fig. 7, we have plotted the CDFs for the ISL expectation (normalized by $r^2[0]$) with respect to different values of $\alpha = \frac{P_s}{P_c}$. We used 256-QAM modulation and 256 subcarriers. We observe that, when α becomes large, the ISL is significantly reduced, which means that the Golomb code based sensing waveform can substantially improve the performance of sensing. An interesting observation is that when α becomes large (greater than 4), the ISL is only slightly reduced. Therefore, it is not necessary to allocate too much power to the sensing waveform.

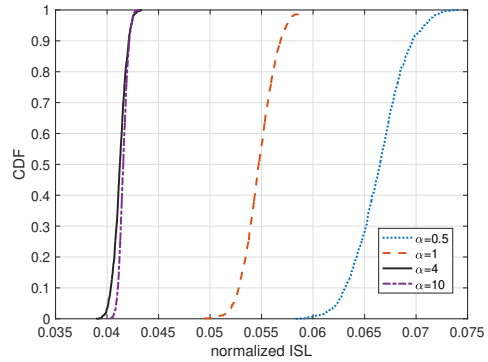

Fig. 7. CDF of ISL for different values of α

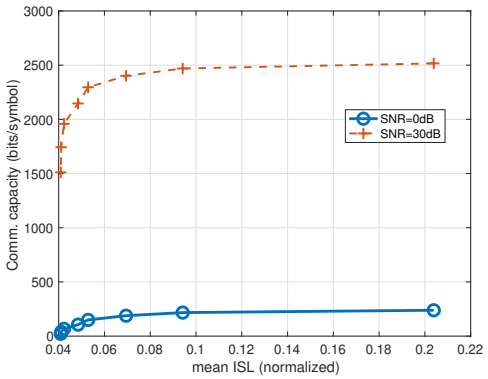

Fig. 8. Trade-off between communications and sensing

C. Trade-off Between Communications and Sensing

The same simulation setup as that in Fig. 7 is used for the simulation in Fig. 8, in which the trade-off is plotted for sensing (in terms of mean ISL) and communications (in terms of channel capacity). The low SNR (0dB) and high SNR (30dB) regimes are considered. The curves are obtained from various values of α (ranging from 0.25 to 16). We observe that, when ISL is greater than a certain value (e.g., 0.08 for the 30dB case), the communication performance is saturated.

D. Performance Gain

We used the simulation setup in Fig. 8 with SNR=0dB, and compared the performance between the proposed dirty paper coding scheme and the scheme of linearly superposition of the sensing and communication waveforms. The trade-off curves for the two schemes are plotted in Fig. 9. We observe that there exists a significant performance gain due to the dirty paper coding.

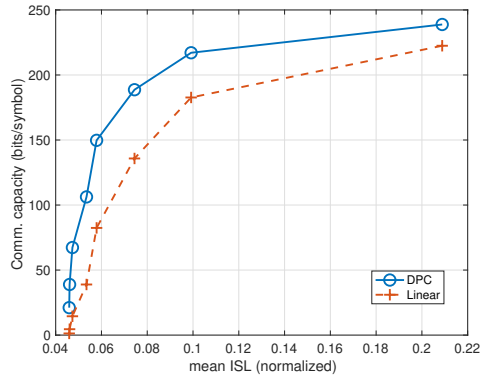

Fig. 9. Comparison between dirty paper coding and linear superposition

VII. Conclusions

In this paper, we have considered the ISAC transmission as a broadcast channel. In the ISAC sensing, deterministic sensing signal is superimposed on the random communication signal. Motivated by the analogy to broadcast channel, we have proposed to leverage the dirty paper coding for removing the interference of the deterministic sensing signal to the communication signal. Numerical simulation results have demonstrated the performance of the proposed ISAC scheme.

References

[1] H. LI, "Performance trade-off in inseparable joint communications and sensing: A pareto analysis," in *submitted to IEEE International Conference on Communications (ICC)*, 2022.

[2] J. L. H. He and P. Stoica, *Waveform Design for Active Sensing Systems: A Computational Approach*. Cambridge University Press, 2012.

[3] M. H. M. Costa, "Writing on dirty paper," *IEEE Trans. on Inform. Theory*, vol. 29, no. 3, 1983.

[4] L. Han and K. Wu, "Joint wireless communication and radar sensing systems–state of the art and future prospects," *IET Microwaves, Antennas & Propagation*, vol. 7, no. 11, pp. 876–885, 2013.

[5] B. Paul, A. R. Chiriyath, and D. W. Bliss, "Survey of rf communications and sensing convergence research," *IEEE Access*, vol. 5, pp. 252–270, 2016.

[6] L. Zheng, M. Lops, Y. C. Eldar, and X. Wang, "Radar and communication co-existence: an overview," *arXiv preprint arXiv:1902.08676*, 2019.

[7] F. Liu, C. Masouros, A. Petropulu, H. Griffiths, and L. Hanzo, "Joint radar and communication design: Applications, state-of-the-art, and the road ahead," *IEEE Transactions on Communications*, 2020.

[8] D. Ma, N. Shlezinger, T. Huang, Y. Liu, and Y. C. Eldar, "Joint radar-communications strategies for autonomous vehicles," *IEEE Signal Processing Magazine*, vol. 37, no. 4, pp. 85–97, 2020.

[9] M. Kobayashi, H. Hamad, G. Kramer, and G. Caire, "Joint state sensing and communication over memoryless multiple access channels," *Proc. of IEEE International Symposium on Information Theory (ISIT)*, pp. 270–274, 2019.

[10] D. W. Bliss and H. Govindosamy, *Adaptive Wireless Communications: MIMO Channels and Networks*. Cambridge University Press, 2011.

[11] K. W. Forsythe, "Utilizing waveform features for adaptive beamforming and direction finding with narrow-band signals," *Lincoln Laboratory Journal*, vol. 10, no. 2, pp. 99–126, 1997.

[12] D. Gaglione, C. Clemente, C. V. Ilioudis, A. R. Persico, I. K. Proudler, J. J. Soraghan, and A. Farina, "Waveform design for communicating radar systems using fractional fourier transform," *Digital Signal Processing*, vol. 80, pp. 57–69, 2018.

[13] K. V. Mishra, M. B. Shankar, V. Koivunen, B. Ottersten, and S. A. Vorobyov, "Toward millimeter-wave joint radar communications: A signal processing perspective," *IEEE Signal Processing Magazine*, vol. 36, no. 5, pp. 100–114, 2019.

[14] D. Tse and P. Vishwanath, *Fundamentals of Wireless Communication*. Cambridge, 2005.

[15] G. Caire and S. Shamai, "On the achievable throughput in multiple antenna gaussian broadcast channel," *IEEE Trans. on Inform. Theory*, vol. 49, no. 7, pp. 1691–1706, 2003.

[16] W. Yu and J. M. Cioffi, "Sum capacity of gaussian vector broadcast channels," *IEEE Trans. on Information Theory*, vol. 50, no. 9, pp. 1875–1892, 2004.

[17] U. Erez and S. ten Brink, "A close-to-capacity dirty paper coding scheme," *IEEE Trans. on Inform. Theory*, vol. 51, no. 10, pp. 3417–3432, 2005.

[18] A. D. L. Y. Sun, M. Uppal, S. Cheng, V. Stankovic, and Z. Xiong, "Nested turbo codes for the costa problem," *IEEE Trans. on Inform. Theory*, vol. 55, no. 3, pp. 388–399, 2008.

[19] B. Schutz, *Lattice Coding for Signals and Networks*. Cambridge University Press, 2009.

[20] H. Li, "Conflict and trade-off of waveform uncertainty in joint communication and sensing systems," in *ready for submission*, 2021.